POTENTIALITIES OF OPTICAL FIBRE BRAGG GRATING SENSORS TO RESIN TRANSFER MOULDING PROCESS MONITORING

Rui de Oliveira, Markus Nordlund, Véronique Michaud and Jan-Anders E. Månson

Laboratoire de Technologie des Composites et Polymères (LTC), Ecole Polytechnique Fédérale de Lausanne (EPFL), CH 1015 Lausanne

ABSTRACT

The feasibility of using fibre Bragg grating (FBG) sensors to monitor the flow progression during RTM, when the resin and the mould are at the same temperature, is investigated. Different sensor locations are considered, as well as four flow rates in order to evaluate their impact on the flow monitoring sensitivity. It is shown that the FBG sensors can easily detect when the resin enters the preform, but it is more difficult to detect the passing flow front. The potential of monitoring the RTM process, obtained from FBG sensors, are discussed in light of the results

1. INTRODUCTION

Resin transfer moulding (RTM) is a widely used process for the manufacturing of composite parts. It is gaining market share comparing with autoclave process in particular for high performance applications, such as aerospace, thanks to its higher versatility permitting the manufacturing of complex and high quality composite parts in fairly short cycle times. The major disadvantage of RTM remains its lack of repeatability in particular for complex shape parts manufacturing. For these, it is not unusual to observe some dry spots and unimpregnated zones.

In RTM process, fibre preforms are placed in a closed mould. Resin is injected to saturate the empty pores in the preform. Resin flow conditions are affected by the resin viscosity, the preform permeability, the applied pressure, the temperature, the reinforcement stacking sequence and the resin infusion strategy. The monitoring of resin flow and its control, from inlets at different position, should lead to an improvement of the process [1].

Different sensors (e.g. dielectric [2], temperature [3], pressure [4], etc.) have been successfully applied to resin flow monitoring, mainly in laboratory applications, for parts with simple geometries. Among theses sensors a particular attention has been dedicated to optical fibre sensors [5-9] due to their good embedding capacity and to the fact that they can be used for structural health monitoring (SHM) during service. Due to the local behaviour of these sensors, they need to be embedded in pre-defined critical structural locations, for their optimised application. However, this location may not correspond to the critical manufacturing zones. This study considers this aspect. This article discusses the added potentialities, for RTM process, when embedding optical fibre Bragg grating (FBG) sensors to design an in-service SHM system having no a priori knowledge of processing disturbance locations. FBG sensors, when applied to resin flow monitoring in RTM, are generally used as temperature sensors (e.g. [8]). Here, the case of RTM at constant flow rate, a low viscosity epoxy resin at the same temperature of the mould is considered. In this case, the flow front cannot be monitored by temperature measurements. Different sensor locations are considered, as well as four flow rates in order to study their impact on flow monitoring. FBG answers are related to flow measurements made by image analysis of video acquisitions. The degree of

reliability of the FBG sensors information on flow front progression during injection is then discussed.

2. FIBRE BRAGG GRATING

FBGs are formed when a permanent periodic variation of the refractive index of the optical fibre core is created, by exposing a section of the optical fibre to an interference pattern of ultra-violet (UV) light [10]. The photosensitivity of germano-silicate glass allows the index of refraction in the core to be changed by the UV laser radiation. When a broadband light source is coupled to the optical fibre containing a FBG, the grating diffractive properties promote that only a very narrow wavelength band is back-reflected.

The centre wavelength of this band, λ_B, can be expressed by the Bragg condition [11]:

$$\lambda_B = 2n\Lambda_B \tag{1}$$

where n is the average effective index of the core and Λ_B is the grating period.

FBG sensors are wavelength-encoded sensors and provide an absolute measurement of the physical perturbation they experience. When the fibre is stretched or compressed along its axis, the period of the grating and n change. The same is observed when the temperature changes. The bare FBG provides a linear response, in a first approximation, based on the measurement of the Bragg wavelength shift:

$$\frac{\Delta\lambda_B}{\lambda_B} = \left\{1 + \left[\frac{1}{n}\frac{\partial n}{\partial \varepsilon}\right]_T\right\}\Delta\varepsilon_{app} + \left\{\alpha_f + \left[\frac{1}{n}\frac{\partial n}{\partial T}\right]_\varepsilon\right\}\Delta T = K_\varepsilon \Delta\varepsilon_{app} + K_T \Delta T \tag{2}$$

where K_ε and K_T are the sensor sensitivities to strain and temperature, respectively, $\Delta\varepsilon_{app}$ is the applied axial strain and ΔT is the temperature variation. The temperature sensitivity K_T is the sum of the silica fibre thermal expansion, α_f and the thermo-optic coefficient, ξ. To recover the strain value, the effect of thermal dependence must be subtracted. The temperature must then be measured separately. This can be done by different methods (e.g. using a thermocouple or a second FBG [12]). For a silica fibre, the FBG wavelength-strain sensitivity at 1555 nm is ~1.15 pm.με^{-1} [10].

3. EXPERIMENTAL PROCEDURE

3.1 Materials

Four different plates constituted of two layers of a unidirectional glass fibre fabric, with area weights of 0.424 kg.m^{-2} each, were fabricated during this study. The fabric permeability, K, was experimentally determined by the methodology described in [13]. Its average value was determined to be $6.6 \cdot 10^{-10}$ m^2.

The resin used was a commercial, thermoset two component system. Its base was a diglycidyl ether of bisphenol (Epikote 828LV epoxy resin from Shell) and the hardener was an isophorone diamine (Epikure DX 6514 from Shell). Data for the epoxy system were given in [14]. The mixing ratio for this system was 100:17 parts by weight of base and hardener, respectively. The injection temperature was 80°C corresponding to a viscosity of around 0.078 Pas.

3.2 FBG sensors

FBGs with a gauge length of 4 mm were written in silica fibres SMF-28e® from Corning. Before UV irradiation, the optical fibre acrylate coating was chemically removed along 8 mm in the FBG zone. Limits of the uncoated zones were underlined

by two red marks to facilitate their visualisation in video records. After fabrication, the FBG sensors were pre-annealed at 100 °C during 24 hours, since the maximum curing temperature of the glass fibre epoxy composite material is of 80°C. This pre-annealing is necessary, in order to ensure the Bragg wavelength temperature stability [15].
Sensors were placed between the two parallel layers in the middle of the composite laminate stack, along the direction of the reinforcement, at different positions as described in Figure 1. For the 2nd plate, a sensor was also used outside of the fabric, to monitor only the resin. FBGs positioning are summarized in Table 1. The optical fibres were pre-stressed and fixed, at two points, to the mould with the tacky tape used to seal the mould.
The variation of the wavelength of the light reflected by the FBG during injection was monitored using an optical sensing interrogator sm125-500 from Micron Optics Inc. Bragg wavelength was recorded at 0.5 Hz. This device uses a tunable multi-mode fibre laser with a 'quasi un-polarized' light output. K-type thermocouples were used to monitor the temperature.

Exp.	**Sensor 1 (x,z) [mm]**	**Sensor 2 (x,z) [mm]**	**Sensor 3 (x,z) [mm]**	**Sensor 4 (x,z) [mm]**	***R* [mm/pixel]**	***Q* [10^7 m^3s^{-1}]**
1	(16.9,10.3)	(20.5,42.6)	(26.2,63.1)		0.1689	3.6
2	(10,10)	(18,33)	(24,58.5)	(30.5,-6)	0.2278	1.1
3	(15.2,10.1)	(19.5,38.3)	(25.2,61.2)		0.2085	2.3
4	(13.9,10.5)	(21.3,35.6)	(25.4,59.7)		0.1878	2.9

Table 1: Sensor position coordinates, spatial resolution and flow rates for the experiments.

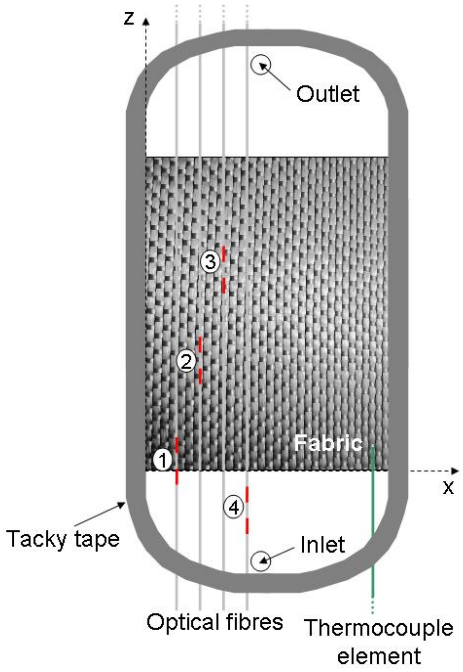

Figure 1: Experimental setup and sensor positioning.

3.3 The mould and injection

The fabrics were stacked into a flat mould consisting of a lower part made out of steel and an upper part made out of glass reinforced by a steel frame (Figure 2). This transparent mould is heated with six evenly distributed computer controlled heat

cartridges, and can withstand temperatures up to 200°C. The temperature of the mould was set to 80°C to ensure a close to constant fluid viscosity for all injections carried out in the present work.

Figure 2. Transparent mould used for the RTM injections

In order to have control of the fibre volume fraction of the tested specimen, the height between the lower and the upper part of the mould was adjusted by inserting metal frames with constant thickness around the lay-up. The dimensions of the injected parts for all the experiments in this work are, 100 × 100 × 0.4 mm^3, leading to a volume fraction, V_f, of around 57.2%. In order to avoid flow racing at the sides of the fabric, the fabric lay-up was sealed with tacky tape. Furthermore, the mould was raised to a vertical position as shown in Figure 2 in order to facilitate video acquisition of the flow front propagation through the transparent upper part of the mould.
Resin system was injected using an Eldo-Mix 101 injection unit from Dopag AG designed to accurately maintain constant flow rates.

3.4 Video acquisition

The video acquisitions of the injection processes were carried out with a Canon PowerShot S70 camera, which acquires 10 frames per second at 30 seconds with a resolution of 640 × 480 pixels. The corresponding resolution in (mm) is calculated by comparing the actual dimensions of the produced sample and its extension in pixels in the acquired image frames. Since the camera position is slightly different between the experiments, the spatial resolution, R (mm/pixel), for each experiment is displayed in Table 1.
In order to correlate the response of the optical sensors on the flow propagation, the video and the optical signal acquisition were synchronized. The sensor locations were determined from photos made at injection end. The arrival time of the resin at the sensors was determined by image analysis of the acquired video frames, as well as the flow rates that were post-calculated from the video acquisition [16]. Values are summarised in Table 1.

4. RESULTS AND DISCUSSION

Figure 3 presents a picture of the propagating flow along the preform. The flow front is not uniform along the fabric width due to the local variation of permeability in the perform and capillary effects.

For the 1st plate the imposed constant flow rate was set to $3.6.10^{-7}$ $m^3.s^{-1}$. Figure 4 presents the variation of the Bragg wavelength for the three sensors which were located at the coordinates presented in Table 1. The temporal reference points: touch of fabric, touch of sensor, end of fabric and stop of machine were determined from video recordings.

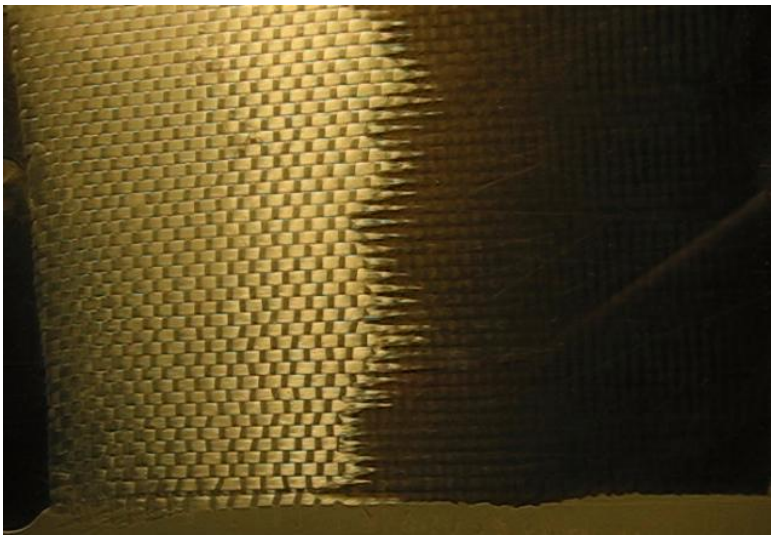

Figure 3: Picture of preform filling, flow is shown from right to left.

The temperature contribution to the variation of the Bragg wavelength was not removed, a single thermocouple being used. A slight difference of 0.5 ºC was observed by the thermocouple between the resin and the mould temperature that caused an increase of around 0.005 nm of central wavelength.

From the curves in Figure 4, it appears that all the three sensors felt simultaneously the moment when the resin touched the fabric and when it reached the end of the fabric. The three sensor exhibited different answers along the injection. Sensor 1 and 2 were in tension whereas the third one seemed to be compressed. The propagating resin may have imposed a curvature to this optical fibre rather than a continuous elongation resulting in the decrease of the central wavelength.

This difference of behaviour was already observed, before initiating the injection, at the end of the mould heating. Whereas the two first sensors indicated a heating of around one degree, the third one indicated a cooling of around 0.5 degree. This difference, along the heating, may be related to the difference in the stress applied at optical fibres pre-stressing and to the fact that the tacky tape at the contact points with the mould may also have flowed differently, for the three optical fibres.

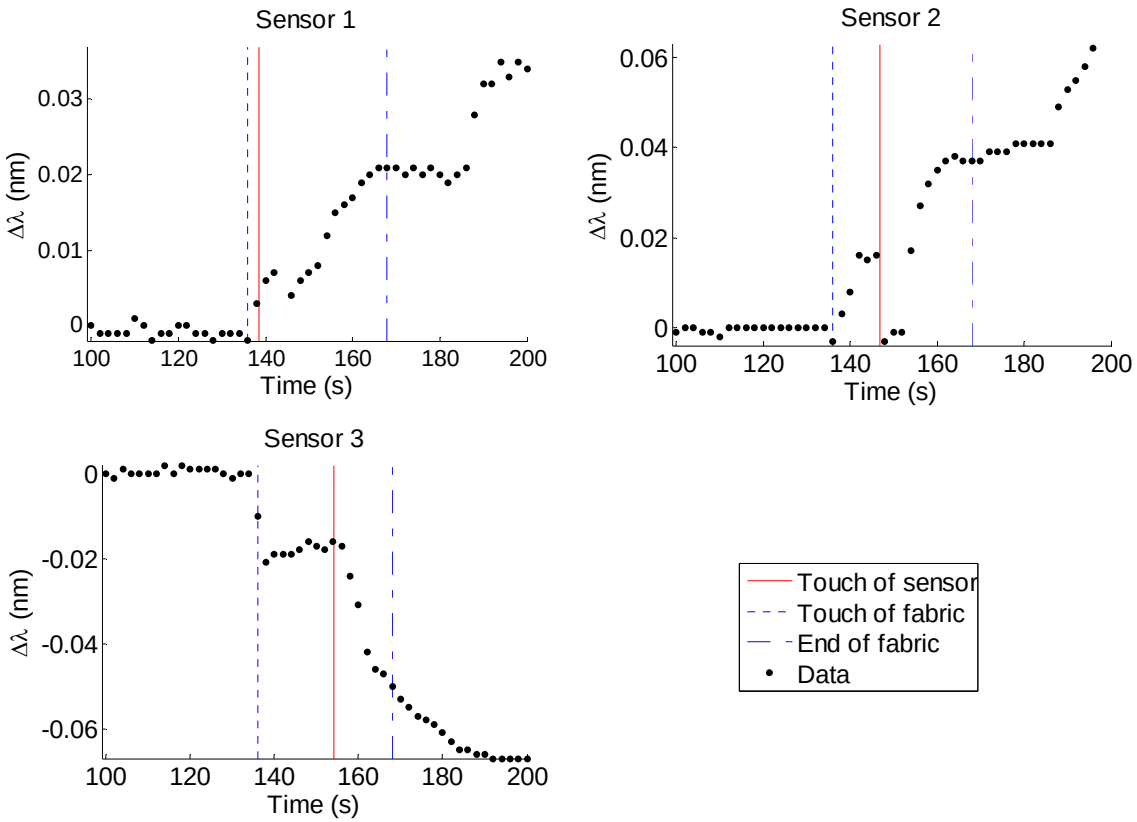

Figure 4: Response of FBGs along variation for plate 1.

The difference of behaviour during the filling process is also due to the presence of the surrounding dry fabric. The simultaneous recording of FBG reflection spectrum during the injection permitted to observe a slight broadening of the central lobe of the spectrum (i.e. up to 10 pm for an original width of 400 pm) for the two first sensors and a slight decrease (i.e. 6 pm for an original width of 340 pm) for the last one. The spectrum broadening is due to micro-bending or compression on the sensor imposed by the microstructure.

Microscope observations were made after composite cure to search for a relation between the difference in the sensor behaviour and their adjustment to the surrounding material. Three final sensor positionings were observed and are summarized in Figure 5. Sensors were either stacked in-between two E glass wefts used for the fabric knitting (e.g. sensor 1), ether at the interface of the UD tow with the glass weft (e.g. sensor 3) or in the middle of the unidirectional reinforcement (e.g. sensor 1 in the 2nd plate). No tendency was observed in the relation between the final sensor positioning and the sensor behaviour during injection process. In Figure 5 (b), the coated optical fibre is visible. It seems that this last has melted during processing despite the fact that the cure temperature is within its operating range [17]. A coating/cladding decohesion is observed. This may result in a worst stress transfer from the fabric to the optical fibre during injection and cure.

The Bragg wavelength (Figure 4) shift value changes from the moment the resin touches the fabric. This change is accentuated at the flow arrival at sensors, the observed difference being higher than the 0.005 nm increase due to temperature. Apparently, in the case of sensors 1 and 2 the optical fibres are slightly stretched at resin arrival in the fabric, this is due to a slippage between the two layers of the fabric

induced by the injected resin. This movement of the fabric is not perceptible from the video recordings as it is in the range of micrometers.
Once covered, the sensors remained affected by the propagating flow as FBG measured the strain along the gauge length, which is defined by the distance between points of contact of the optical fibre with the fabric. The propagating resin moves this contact point along the optical fibre. FBG can thus indicate the sliding or potential shear of the fabric due to the propagating resin. This is observed until the resin reaches the end of the fabric. For the sensor 3 the same trends were observed but for negative difference on the central wavelength.

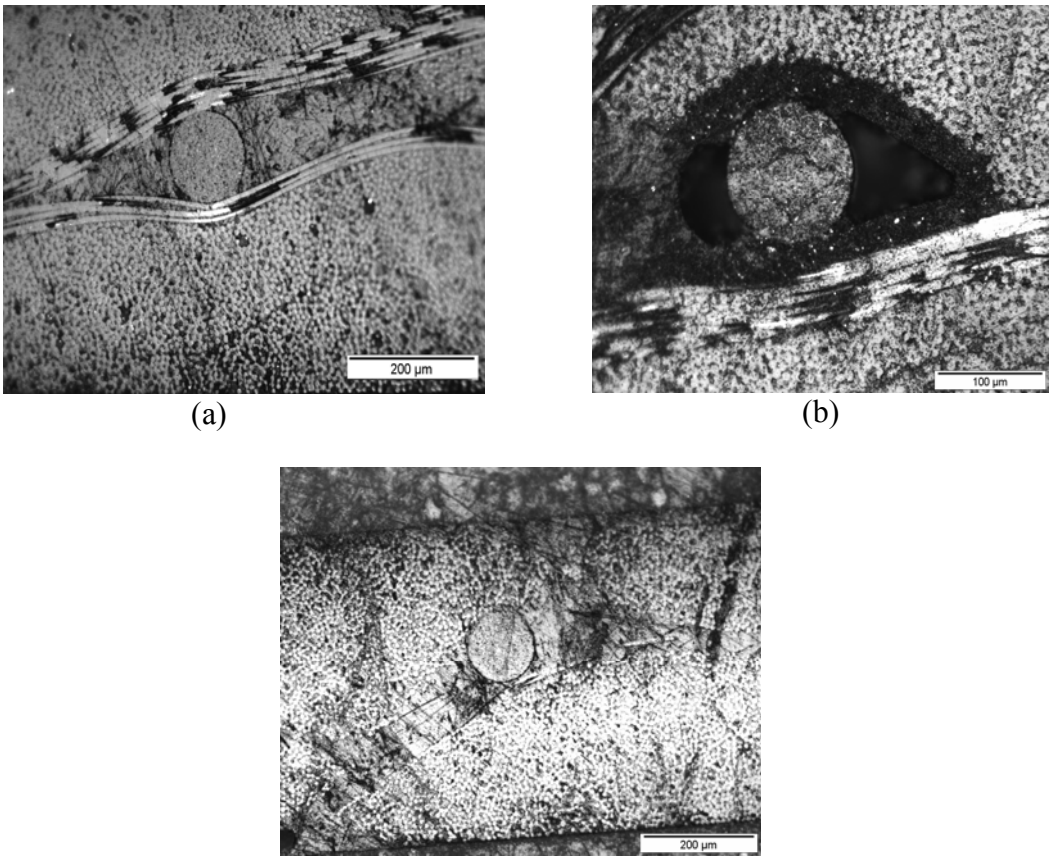

(a) (b)

(c)

Figure 5. Microscope observation of embedded (a) sensor 1 – plate 1, (2) sensor – plate 1, (3) sensor 1 - plate 2.

The use of a lower flow rate did not cause any significant effect on the amount of wavelength variation (e.g. for the 2nd plate in Figure 6). The resin arrival at the fabric and at its end is less pronounced for the lower flow rates. For the 3rd and 4th plate all sensors exhibited a similar behaviour to that of sensor 3 in the 1st plate. Comparing the slope of the wavelength shift for the different flow rates no apparent relation was observed.
In the case of 2nd plate, a FBG was positioned before the fabric (sensor 4 in Figure 1), during manufacture, to dissociate the component of the induced stresses on the optical fibre due to the resin from the contribution of the fabric. The resin arrival at sensor could not be determined from this FBG. At that point, the strain is transferred to the FBG through shear stresses. The transfer depends on the resin viscosity, which is apparently too low in this application. This sensor could however notice the resin arrival at the fabric and a constant increase of the wavelength was observed until 114

seconds of injection. At that point, the wavelength slowly decreased until injection stopped. This confirms that the wavelength changes experienced by the sensors are mainly due to the movement of the fabric. The wavelength decrease from 114 seconds is probably due to a rearrangement of the fabric around the optical fibre. Similar trend was observed for the sensor 3 at 108 seconds.

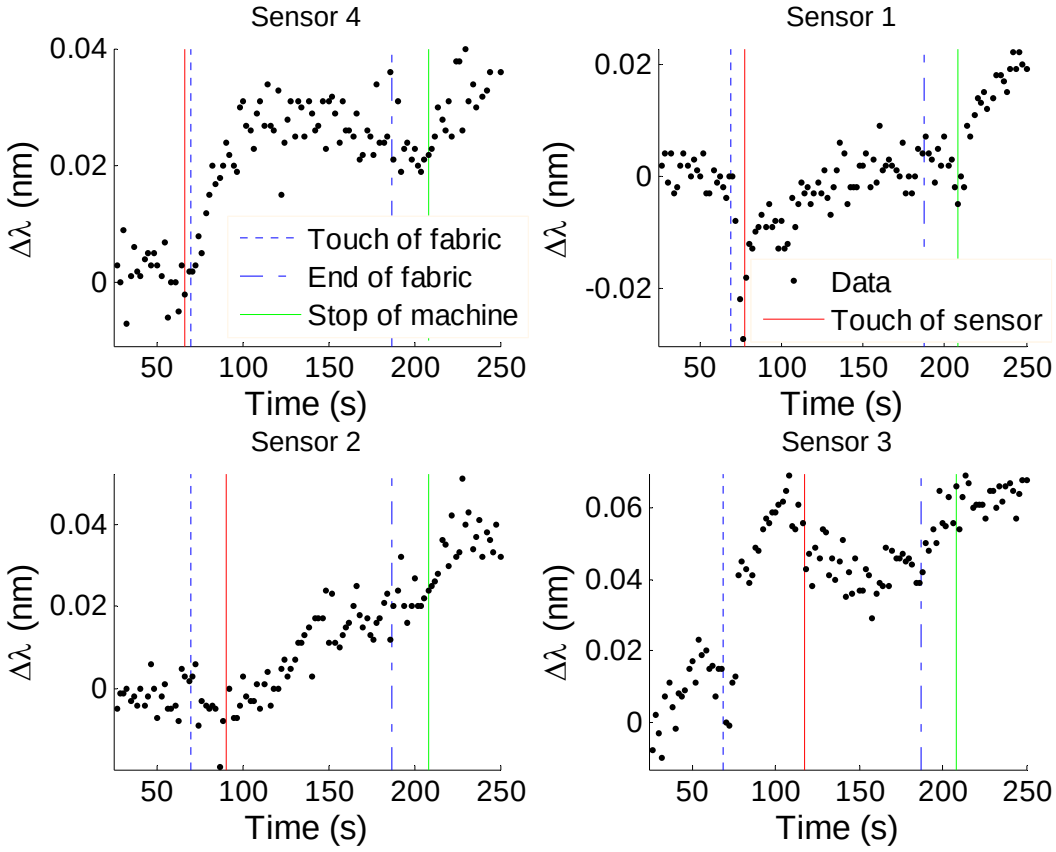

Figure 6. Response of FBGs along variation for plate 2.

5. CONCLUSION

The goal of this study was to verify the capacity of FBG to monitor the flow front propagation during RTM process when the resin and the mould are at the same temperature and for a low viscosity resin system.

Relating the variation of Bragg wavelength to the flow front propagation measurements made from video image analysis confirmed that FBG sensors can be used for that purpose. All FBG sensors in the preform detected, simultaneously, the arrival of the resin at the fabric, independently of their location, from the fabric layer movement when pushed by the propagating resin. However, depending on the initial condition applied to the optical fibre (i.e. pre-stress amount, contact condition to the fabric and mould, temperature) and its interaction with the fabric during the injection, the sensor exhibits different behaviours (i.e. increase or decrease of wavelength). The flow rate showed to have also an effect on the sensitivity of the FBG sensor to the flow front progress. FBG sensors could however not be used to quantify the flow rate.

ACKNOWLEDGEMENTS

R. de Oliveira would like to thank the Portuguese Foundation for Science and Technology (FCT) for financial support. Dr. Costantini from Advanced Photonics

Laboratory at EPFL and Maxime Govaerts, from LTC, are thanked for advice and assistance.

REFERENCES

1. Hsiao K.T., Advani S.G., "Flow sensing and control strategies to address the race-tracking disturbances in resin transfer molding—Part I: design and algorithm development", *Composites Part A*, vol. 35, pp. 1149–1159, 2004.
2. Skordos A.A, Karkanas P.I., Partridge I.K, "A dielectric sensor for measuring flow in resin transfer moulding", *Measurement Science and Technology*, vol. 11, pp. 25–31, 2000.
3. Sozer E.M., Tuncol G., Danisman M., Kaynar A., "Constraints on monitoring resin flow in the resin transfer molding (RTM) process by using thermocouple sensors", *Composites Part A*, vol 38, pp. 1363-86, 2007.
4. Parthasarathy S., Mantel S.C., Stelson K.A., Bickerton S., Advani S.G., "Real-time sensing and control of resin flow in liquid injection molding processes", *Proceedings of the American Control Conference Philadelphia*, Pennsylvania June 1998
5. Lekakou C., Cook S., Deng Y., Ang T.W., Reed G.T., "Optical fibre sensor for monitoring flow and resin curing in composites manufacturing", *Composites: Part A*, vol. 37, pp. 934–938, 2006
6. Dunkers J.P., Lenhart J.L., Kueh S.R., van Zanten J.H., Advani S.G., Parnas R.S., "Fiber optic flow and cure sensing for liquid composite molding", *Optics and Lasers in Engineering,* vol. 35, pp. 91-104, 2001.
7. Yoon Y., Jeong S., Lee W., Lee B., "A Study on the measurement technique of resin flow and cure during the vacuum assisted resin transfer moulding process using the long period fiber bragg grating sensor", *Advanced composites letters,* vol. 13, pp. 237-243, 2004.
8. Novo C., Frazão O., Costa A.N., Vieira A., Correia N., Dias I., Araújo F.M., Marques A.T., "Progression monitoring of the flow front in RTM process using fibre Bragg grating sensors", *Proceedings of the 14th International Conference on Optical Fiber Sensors, SPIE*, vol. 4185, pp. 808-11, 2000.
9. Eum S.H., Kageyama K., Murayama H., Ohsawa I., Uzawa K., Kanai M., Igawa H., "Resin Flow Monitoring in Vacuum Assisted Resin Transfer Molding Using Optical Fiber Distributed Sensor", *SPIE*, vol. 6526, p. 65262T-1, 2007.
10. Morey A.W., Meltz G., Glenn W., "Fibre optic bragg grating sensors", *Fiber Optic and Lasers Sensors VII*, vol. 1169, pp. 98-107, 1989.
11. Kersey A.D., Davis M.A., Patrick H.J., Le Blanc M., Koo K.P., Askins C.G., Putnam M.A., Friebele E.J. "Fiber grating sensors", *J Lightwave Technol*, vol. 15, pp. 1442-1463, 1997.
12. Yoon H.J., Costantini D., Limberger H.G., Salathé R., Kim C.G., Michaud V., "In-situ strain and temperature monitoring of adaptive composite materials", *J Intell Mater Struct*, vol. 17, pp. 1059-1067, 2006.
13. Verrey J., "Resin transfer moulding of complex shaped composites using carbon fibre non-crimp fabrics", PhD thesis EPFL, 2004.
14. Lee H., NevilleK., "Handbook of Epoxy Resins", 1st ed. McGraw-Hill, 1967.
15. Kannan S., Guo J.Z.Y., Lemaire P.J., "Thermal stability analysis of UV induced fiber Bragg gratings", *J Lightwave Technol*, vol 15, pp. 1478-1483, 1997.

16. Nordlund M., Michaud V., Månson J.-A.E., “Dynamic saturation curve measurements during resin flow in glass fibre reinforcements”, *Composites part A*. Submitted for publication, 2008.
17. Corning® SMF-28® optical fibre. Product information. http://www.corning.com /docs/opticalfiber/pi1344.pdf